

# Interference Management via Sliding-Window Coded Modulation for 5G Cellular Networks

Kwang Taik Kim, Seok-Ki Ahn, Yong-Seok Kim, Jeongho Park, Chiao-Yi Chen, and Young-Han Kim

SWCM aims to mitigate the adverse effects of interference at the physical layer by tracking the optimal maximum likelihood decoding performance with low-complexity decoding and minimal coordination overhead. The authors review the basic structure of the SWCM scheme built on the principles of network information theory, and discuss how it can be extended and implemented in practical wireless communication systems.

## ABSTRACT

SWCM aims to mitigate the adverse effects of interference at the physical layer by tracking the optimal maximum likelihood decoding performance with low-complexity decoding and minimal coordination overhead. This article reviews the basic structure of the SWCM scheme built on the principles of network information theory, and discusses how it can be extended and implemented in practical wireless communication systems. Using a representative implementation based on LTE OFDM MIMO systems, extensive link-level and system-level performance simulations are carried out, which demonstrate that SWCM offers significant gains for all users over conventional interference-aware communication schemes. Network operating prerequisites for SWCM are also discussed to facilitate the standardization effort for its adoption in the fifth generation cellular network.

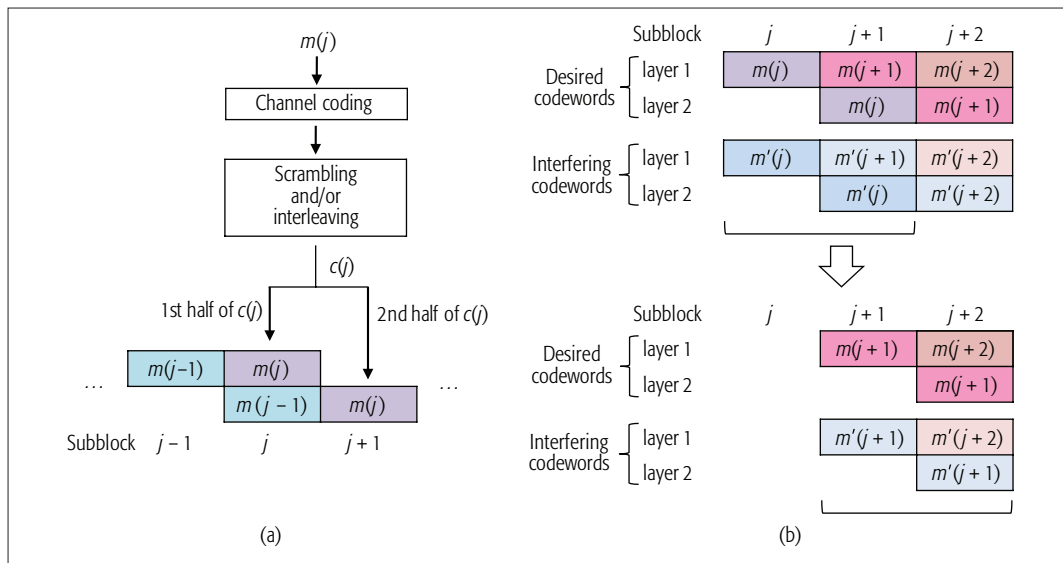
## INTRODUCTION

According to the Third Generation Partnership Project (3GPP) study on scenarios and requirements for next-generation access technologies [1], the cell edge performance (typically measured by the spectral efficiency of the 5th-percentile user) of the fifth generation (5G) mobile network must be at least three times higher than that of IMT-Advanced. This cell edge performance, one of the key performance indicators of 5G, is crucially affected by co-channel interference from neighboring cells, which becomes more severe as small cells are deployed more densely in 5G. Consequently, proper mitigation of the performance degradation due to interference becomes one of the key challenges in the 5G radio access network. As a first step in addressing the co-channel interference problem on the receiver side, conventional linear receivers have been improved by incorporating statistical information on interference channels as in linear minimum mean square error interference rejection combining (LMMSE-IRC) receivers [2, 3], which are now widely used in commercial systems. As a next step, network assisted interference cancellation and suppression (NAICS) has been proposed, first as a study/work item for the 3GPP Long Term Evolution-Advanced (LTE-A) in Release 12, in which several types of interference-aware receivers and control signal-

ing for them were discussed. As a result of the standardization of NAICS [4], symbol-level interference-aware detection (IAD) [5] is expected to be implemented in many commercial receivers in the near future.

In network information theory, several decoding techniques have been studied for point-to-point (P2P) random codes over interference channels. Among these, treating interference as Gaussian and discrete noise roughly corresponds to LMMSE-IRC and IAD, respectively. Treating interference as noise, despite its advantage of low-complexity implementation, typically suffers from a significant rate loss when the interference signal strength at the receiver is moderate to high. In comparison, sequence-level interference-aware decoding such as information-theoretic simultaneous nonunique decoding (SND) can asymptotically achieve the rate region of the optimal maximum likelihood decoding (MLD) [6, references therein]. Despite this performance advantage, however, MLD and SND rely on some form of multiuser sequence detection, which cannot be implemented in practice due to its high complexity. The question then naturally arises as to how one can achieve the MLD/SND performance at low complexity, which would be the ultimate goal of physical-layer interference management.

A few approaches have been proposed recently to tackle this problem. First, instead of conventional P2P codes such as low-density parity check (LDPC) and turbo codes, one can utilize novel error correcting codes such as spatially coupled codes and polar codes adapted to simultaneous decoding of desired as well as interfering codewords. The resulting multiuser codes [7, 8], however, are often of very long block lengths, not suitable for typical wireless applications. Second, by tweaking decoding steps for conventional turbo codes, one can iteratively decode for both desired and interfering codewords. This interference-aware successive decoding (IASD) scheme [9] performs well in general and better than noniterative successive interference cancellation decoding in particular. However, the IASD scheme still falls short of achieving the MLD/SND performance, especially under a moderate interference level. Third, by transmitting codewords over multiple layers and multiple subblocks, one can achieve the MLD/SND per-



As its name suggests, a receiver in the SWCM scheme recovers desired messages by sliding the decoding window over multiple subblocks. In each decoding window, the desired codeword and/or the interfering codeword is recovered successively.

**Figure 1.** Basic SWCM encoder and decoder structures: a) basic encoder structure with each message transmitted over two layers and two subblocks. The (scrambled and/or interleaved) codeword  $c(j)$  carries message  $m(j)$ ; b) basic decoder structure with sliding-window decoding and successive cancellation decoding. To recover both the desired codeword  $c(j)$  and the interfering codeword  $c'(j)$ , the receiver applies successive cancellation decoding according to a particular decoding order.

formance for P2P random codes using low-complexity successive cancellation decoding. This sliding-window superposition coding (SWSC) scheme [10, 11] is built on basic components of network information theory, carefully combining the ideas of block Markov coding, sliding-window decoding (both commonly used for multihop relaying and feedback communication), superposition coding without rate splitting (codewords mapped into multiple layers), and successive cancellation decoding (codewords recovered one by one). This conceptual coding scheme has been further developed into an implementable coded modulation scheme, whereby conventional binary codes (LTE turbo codes, to be specific) are mapped to transmitted symbols in staggered subblock layering and recovered successively in sliding decoding windows at the receivers [12, 13]. Even under simple bit-mapping rules and hard decision decoding, this sliding-window coded modulation (SWCM) scheme closely tracks the MLD/SND performance for two-user-pair Gaussian interference channels, with significant performance gain over LMMSE-IRC and IAD.

The goal of this article is twofold. First, we review the basic structure of SWCM and present how it can be enhanced and adapted to practical multiple-input multiple-output (MIMO) transceivers in cellular wireless networks. In particular, we discuss how SWCM can be implemented under typical LTE orthogonal frequency-division multiplexing (OFDM) resource allocation and MIMO transmission/reception scenarios. Second, we provide an extensive study on the performance of SWCM for plausible use cases, and demonstrate the performance gain over the aforementioned LMMSE-IRC, IAD, and IASD schemes. At the link level, we evaluate the performance of SWCM for the  $2 \times 2$  MIMO Ped-B fading channel [14] under varying signal-to-noise ratios. At the system level, we simulate a macro urban environment network under 3GPP Release

12 NAICS assumptions, and measure average and cell edge throughput performance. In both cases, SWCM achieves significant performance gain over the existing schemes.

The rest of the article is organized as follows. The next section explains the basic structure of the SWCM scheme and its enhancement for adaptive transmission and reception. The following section demonstrates how the scheme can be implemented in practical OFDM MIMO systems. We then compare the performance of SWCM and competing schemes via link-level and system-level simulations, respectively. The next section discusses necessary network-side operations to enable interference-aware transmitters and receivers based on SWCM. The final section concludes the article.

## SLIDING-WINDOW CODED MODULATION

### BASIC ENCODER AND DECODER STRUCTURES

In the SWCM scheme, a single communication block consists of multiple, say  $b$ , subblocks, each consisting of  $n$  transmitted symbols. Each transmitted symbol is assumed to be decomposable into multiple layers; for example, a 16-quadrature amplitude modulation (QAM) symbol can be viewed as a combination of two 4-QAM layers, two 4-phase amplitude modulation (PAM) layers, or four binary phase shift keying (BPSK) layers. Each message is transmitted over multiple subblocks and multiple layers. Figure 1a illustrates the encoder structure in which each message is transmitted over two layers and two subblocks. To be concrete, we assume that a 4-PAM signal is transmitted, represented as a weighted superposition of two BPSK layers. To communicate the message  $m(j)$  for  $j = 1, 2, \dots, b - 1$ , the encoder uses a binary channel code of length  $2n$  bits to form a codeword and its scrambled (and interleaved, if needed) version  $c(j)$ . For transmission in subblock  $j$ , the second half of

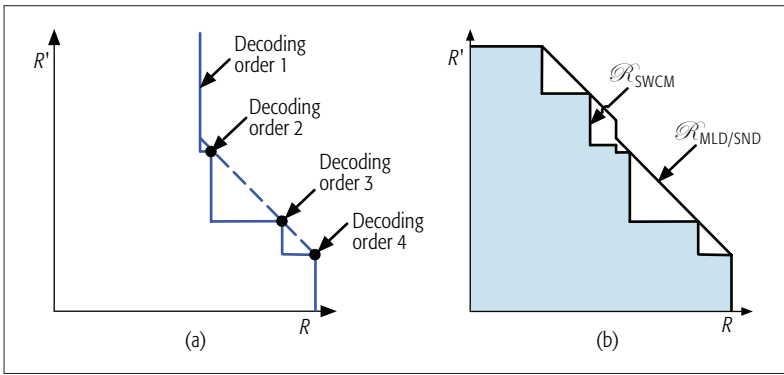


**Figure 2.** SWCM and MLD/SND achievable rate regions: a) SWCM and MLD/SND achievable rate regions at a receiver. The dotted diagonal line reflects the optimal MLD/SND rate region; b) SWCM and MLD/SND achievable rate regions of a system with two sender-receiver pairs. The SWCM region  $\mathcal{R}_{\text{SWCM}}$  is the shaded inner region, while the MLD/SND region  $\mathcal{R}_{\text{MLD/SND}}$  is the nonconvex polytope outer region.

the codeword  $c(j - 1)$  from the previous message  $m(j - 1)$  is mapped to one BPSK layer, while the first half of the codeword  $c(j)$  from the current message  $m(j)$  is mapped to the other BPSK layer. Thus, the superposition of the two BPSK layers, which contains partial information of two messages,  $m(j - 1)$  and  $m(j)$ , forms a sequence of  $n$  4-PAM symbols to be sent in subblock  $j$ . Overall,  $(b - 1)$  messages are transmitted over  $b$  subblocks with one BPSK layer each missing during the initial and final subblocks, resulting in a slight rate loss from the actual code rate. A similar structure can easily be adapted for other transmission symbols, such as higher-order PAM/QAM and PSK symbols. It is worthwhile to point out the key difference in the encoder structure between SWCM and widely used bit-interleaved coded modulation (BICM). The latter is equivalent to mapping the scrambled codeword to BPSK layers transmitted in the same subblock, while in SWCM the scrambled codeword is mapped to BPSK layers over multiple subblocks in a staggered manner. This structure allows SWCM to mitigate interference within a codeword and from other codewords more efficiently, but it suffers the aforementioned rate loss (the larger  $b$ , the better) as well as error propagation over multiple subblocks (the smaller  $b$ , the better).

Each message is transmitted over multiple subblocks and multiple layers. As its name suggests, a receiver in the SWCM scheme recovers desired messages by sliding the decoding window over multiple subblocks. In each decoding window, the desired codeword and/or the interfering codeword is recovered, successively. Figure 1b illustrates an example of the decoding operation that corresponds to the encoder structure in Fig. 1a. In the decoding window spanning over subblocks  $j$  and  $j + 1$ , the receiver recovers the desired codeword  $c(j)$  (using a conventional P2P decoder) and the interfering codeword  $c'(j)$  (again using a conventional P2P decoder) successively. It then slides the decoding window to subblocks  $j + 1$  and  $j + 2$ . Note that successive cancellation decoding is performed within and across decoding windows. If both the desired and interference encoders use the two-layer SWCM

encoder structure illustrated in Fig. 1a, there are four possible decoding orders at a receiver:

1. The desired codeword  $c(j)$  only
2.  $c(j)$ , then the interfering codeword  $c'(j)$
3.  $c'(j)$ , then  $c(j)$
4. The next interfering codeword  $c'(j + 1)$ , then  $c(j)$

with different trade-offs between the rate  $R$  of the desired codeword and the rate  $R'$  of the interfering codeword. Figure 2a illustrates the resulting achievable rate region of  $(R, R')$  and compares it with the optimal MLD/SND achievable rate region; see [10, 11] for the detailed information-theoretic analysis. When two sender-receiver pairs are communicating over an interference channel, the intersection of the achievable rate regions at both receivers determine the achievable rate region of the entire system, as illustrated in Fig. 2b.

### ADAPTIVE TRANSCIEVER DESIGN TECHNIQUES FOR SWCM

The SWCM scheme discussed in the previous subsection can be enhanced to improve performance and robustness in a broad range of channel conditions to satisfy the desired quality of service (QoS) [13]. The basic SWCM encoding structure can be modified in several ways to increase achievable rates. First, one can adaptively control the number of superposition layers for both transmit points (TPs), which provides multiple code rate options by changing the shape of the corner points of the SWCM achievable rate region in Fig. 2b. Second, one can select various bit mapping rules at each TP, which allows different rate points to be achieved in Fig. 2b for the desired QoS. Third, one can assign different power allocation parameters between superimposed layers, which can potentially enlarge both MLD/SND and SWCM achievable rate regions.

The SWCM decoding structure can be modified in multiple ways to improve robustness under channel state information (CSI) mismatch. First, the decoding order (Fig. 2b) can be switched from one to another as the channel condition changes. Second, “soft” information can be utilized instead of “hard” information in each stage of successive cancellation decoding by storing log-likelihood ratios (LLRs) from the decoder output, which can then be used to calculate LLRs for the decoder input in the next stage. Third, iterative decoding, in addition to successive cancellation decoding, can be used; for instance, iterative decoding can be performed throughout the entire block (subblocks 1 through  $b$ ), which can better track the optimal MLD/SND performance.

### IMPLEMENTATION TECHNIQUES OF SWCM

As a coded modulation scheme that interfaces channel coding (typically binary) and physical-layer modulation, SWCM can be applied to different radio access technologies. In this section, we present a representative implementation for LTE OFDM MIMO systems using turbo codes.

#### MULTIPLE-INPUT MULTIPLE-OUTPUT

We modify the architecture of the MIMO transmission system in the LTE standard with three key changes to implement an SWCM MIMO

The SWCM scheme can increase spectral efficiency and reduce decoding error rates over conventional schemes, by utilizing the layered signaling and staggered transmission structure.

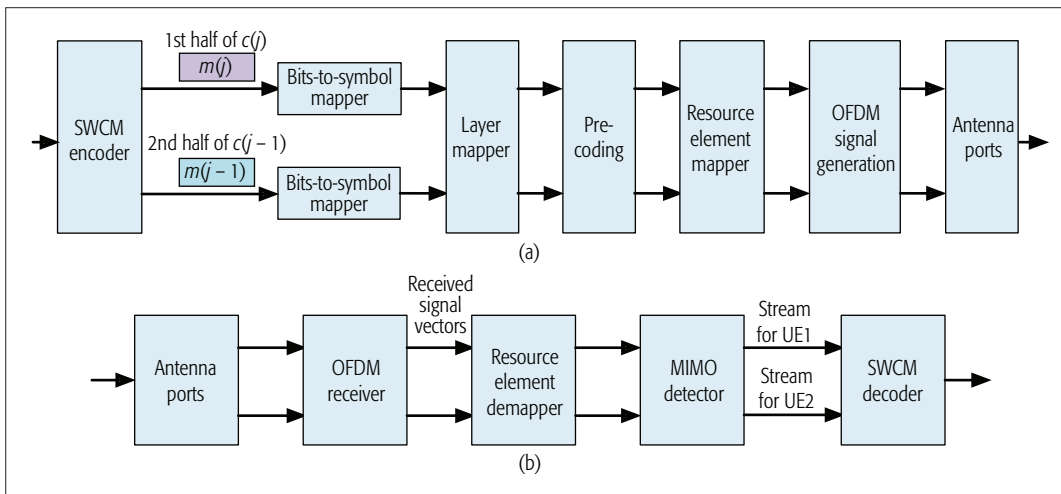


Figure 3. The SWCM MIMO system architecture: a) SWCM encoder, layer mapper, precoder, and resource element mapper for MIMO transmission; b) interference-aware MIMO detector and SWCM decoder.

system architecture. For simplicity, we explain these changes with an SWCM scheme using two layers for a 2Tx–2Rx antenna configuration as shown in Fig. 3, under the assumption that a single stream is communicated. Note that this illustrative design can readily be extended to multiple streams.

First, SWCM replaces BICM over QAM as the coding and modulation mapper. Unlike BICM, any of QAM, PAM, and PSK may be used as an SWCM layer to accommodate flexibility in symbol mapping. To be concrete, assume throughout this subsection that two SWCM layers use two 4-QAM or 4-PAM symbols as a pair. To send the message  $m(j)$  for  $j = 1, 2, \dots, b-1$ , the encoder uses a (binary) LTE turbo code of length  $4n$  bits to form a scrambled codeword  $c(j)$ . This is in comparison to the codeword of length  $2n$  bits used for two BPSK layers as in the previous section. For transmission in subblock  $j$ , the second half of the previous codeword  $c(j-1)$  is mapped to one 4-QAM (or 4-PAM) layer, while the first half of the current codeword  $c(j)$  is mapped to the other 4-QAM (or 4-PAM) layer. The two 4-QAM (or 4-PAM) layers are fed into the layer mapper. A similar procedure can readily be adapted to binary or higher-order PSK and higher-order QAM/PAM symbols.

Second, the layer mapper takes a symbol pair from the two layers to form an input to the precoder. There are two operation modes in the layer mapper: the transmit diversity mode and the spatial multiplexing mode. In the transmit diversity mode, the layer mapper combines one symbol each from the two layers to form a scalar QAM symbol input to the precoder. If the two layers use 4-QAM symbols, the 4-QAM symbol from one layer is superimposed on the 4-QAM symbol from the other layer to form a 16-QAM symbol. If the two layers use 4-PAM symbols, the pair of PAM symbols are taken as in-phase and quadrature components of a 16-QAM symbol. In the spatial multiplexing mode, the layer mapper simply takes two 4-QAM symbols from the two layers to form a vector input to the precoder.

Third, the precoder uses beamforming matrices ( $2 \times 1$  in the transmit diversity mode and  $2$

$\times 2$  in the spatial multiplexing mode) to achieve the best performance under the SWCM encoding/decoding structure instead of interference as noise (IAN) as in LTE. As the output of the precoder, two sequences of  $n$  complex symbols are sent in subblock  $j$  via two antenna ports for  $j = 1, 2, \dots, b$ .

#### FRAME STRUCTURE AND RESOURCE ALLOCATION

As in the LTE standard, the scheduler allocates resource blocks (RBs) or resource elements (REs) in a subframe to one or more UE. To be concrete, assume that  $nb = 1200$  physical REs are allocated to a UE for SWCM transmission in a subframe. Physical REs are mapped to virtual REs by pseudorandom interleaving for frequency diversity. The corresponding 1200 virtual REs are divided into  $b = 10$  subblocks, each can carry  $n = 120$  4-QAM or 16-QAM symbols. The size of a SWCM subblock (480 bits for the entire codeword when 4-QAM or 4-PAM layers are used) is well within the maximum range of the quadratic permutation polynomial (QPP) interleaver, which is 6144 for the LTE turbo code.

#### LINK-LEVEL PERFORMANCE

As expected from the corresponding results in network information theory [6, 10], the SWCM scheme can increase spectral efficiency and reduce decoding error rates over conventional schemes, by utilizing the layered signaling and staggered transmission structure. First, layered signaling enables more flexible decoding of some layers of the codeword from another UE, achieving higher rates than nonlayered schemes. Second, staggered transmission allows a longer codeword to be sent over multiple layers, achieving diversity and robustness for decoding, as either the desired or interference signal, at different receivers. This section presents link-level performance simulation results to demonstrate these benefits quantitatively.

We consider the two-user-pair  $2 \times 2$  symmetric MIMO interference channel model with International Telecommunication Union (ITU) Ped-B fading and additive Gaussian noise under

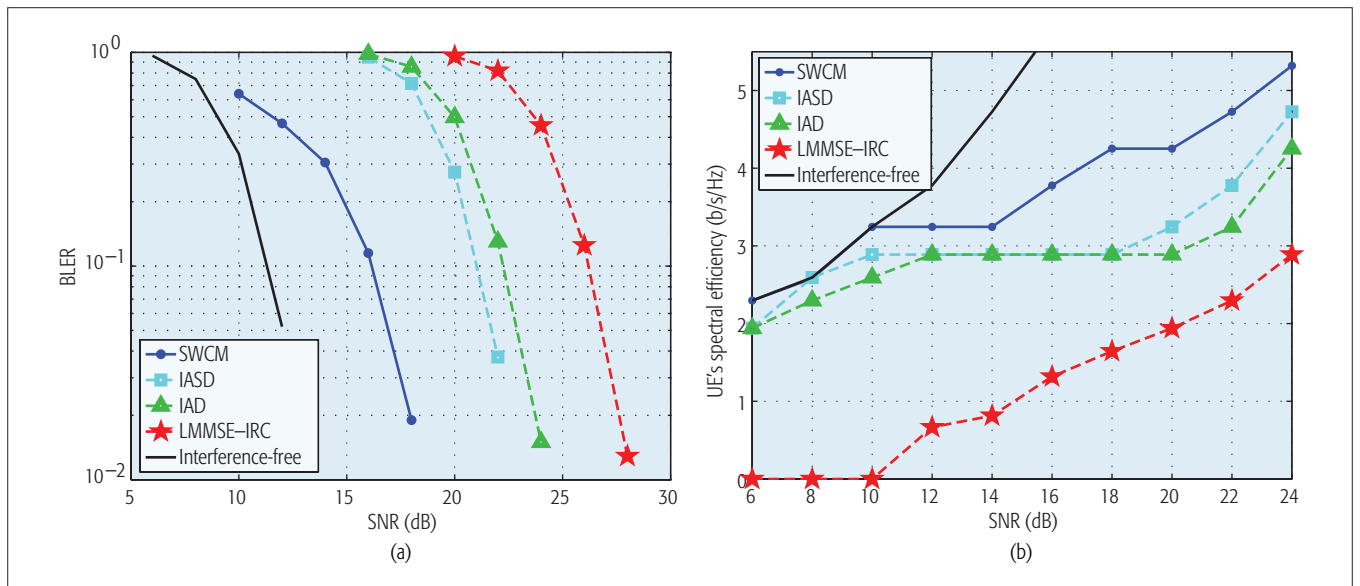


Figure 4. Link-level performance for the 2/2-layer SWCM MIMO scheme with adaptive iterative soft decoding, IASD, IAD, and LMMSE-IRC in the  $2 \times 2$  MIMO symmetric Ped-B interference channel with average received INR = 15 dB: a) BLER vs. average received SNR at MCS 13 (16-QAM) and RI = 2; and b) achievable UE rates vs. average received SNR at BLER = 0.1 and RI = 2.

the 3GPP LTE standard subframe structure [15] and resource allocation described in the previous section. Ped-B channel gains for an OFDM symbol of the subframe over 2048 subcarriers are obtained by taking a fast Fourier transform of six Rayleigh distributed multipath channel taps [14]. The Jakes model is used for time correlation of the channel gains due to pedestrian mobility (3 km/h in the Ped-B channel model) between OFDM symbols of 32.5 ns duration. The channel gains for all links are generated by applying this process independently. The average signal-to-noise ratio (SNR) (or interference-to-noise ratio [INR]) is defined as the ratio of the average received power of the sum of six multipath signals of the desired codeword (or the average received power of the sum of six multipath signals of the interference codeword) to the average power of the noise at the receiver.

The transmitter uses the single-stream two-layer SWCM scheme with an identity matrix (in the spatial multiplexing mode) as the precoder by mapping the sequence of each SWCM layer directly to each precoder output in order to evaluate its simplest open loop spatial multiplexing performance. The block length of SWCM is matched to that of IASD, IAD, and LMMSE-IRC. The receiver uses the adaptive iterative soft decoding technique with eight iterations for each codeword (the same number of iterations used for other schemes to be compared).

We evaluate the performance of SWCM and existing schemes in the  $2 \times 2$  MIMO Ped-B interference channel with average INR of 15 dB. As shown in Fig. 4a, simulation results for the SNR gain at block error rate (BLER) of 0.1 demonstrate that the SWCM scheme outperforms LMMSE-IRC [2, 3] (now widely used in commercial systems) by 10.1 dB, IAD [5] (Release 12 NAICS receiver) by 6.1 dB, and IASD [9] (one of the most advanced interference-aware receivers prior to SWCM) by 4.9 dB. As shown

in Fig. 4b, simulation results for the achievable UE rates under symmetric QoS, again at BLER of 0.1, demonstrate that the SWCM scheme outperforms LMMSE-IRC, IAD, and IASD over all SNR regimes, when the best modulation and coding scheme (MCS) is chosen for each scheme at a given SNR. At the same time, for each fixed MCS, SWCM uniformly outperforms the other schemes (data not shown). For example, SWCM outperforms IAD and IASD by 47 percent and LMMSE-IRC by 159 percent at the average SNR of 18 dB.

## SYSTEM-LEVEL PERFORMANCE

The improved link-level performance does not necessarily translate to a system-wide throughput gain of the same magnitude, since the scheduler based on proportional fairness (PF) metrics may not always select a UE with a channel that has a moderate to high interference level, and thus the performance would benefit greatly from interference-aware decoding as shown in the previous section. In this section, we present simulation results for system-level performance gains of SWCM over conventional schemes, which partly answer the question of to what extent the promising link-level performance of SWCM can carry over to that of the entire network.

Since there is no system specification for 5G yet, we carry out the system-level performance simulation based on 3GPP Release 12 NAICS evaluation assumptions [4]. In particular, we consider NAICS scenario 1, a wrap-around homogeneous macro network with 19 hexagonal cells (3 sectors per cell) and use the 2D spatial channel model (SCM) with a 2Tx-2Rx cross polarized antenna configuration for urban macro (UMa) scenarios between a TP and a UE moving at 3 km/h. The system bandwidth is 10 MHz, and a file transfer protocol traffic model is used for a partial-load scenario. UEs feed back wideband channel quality indicator

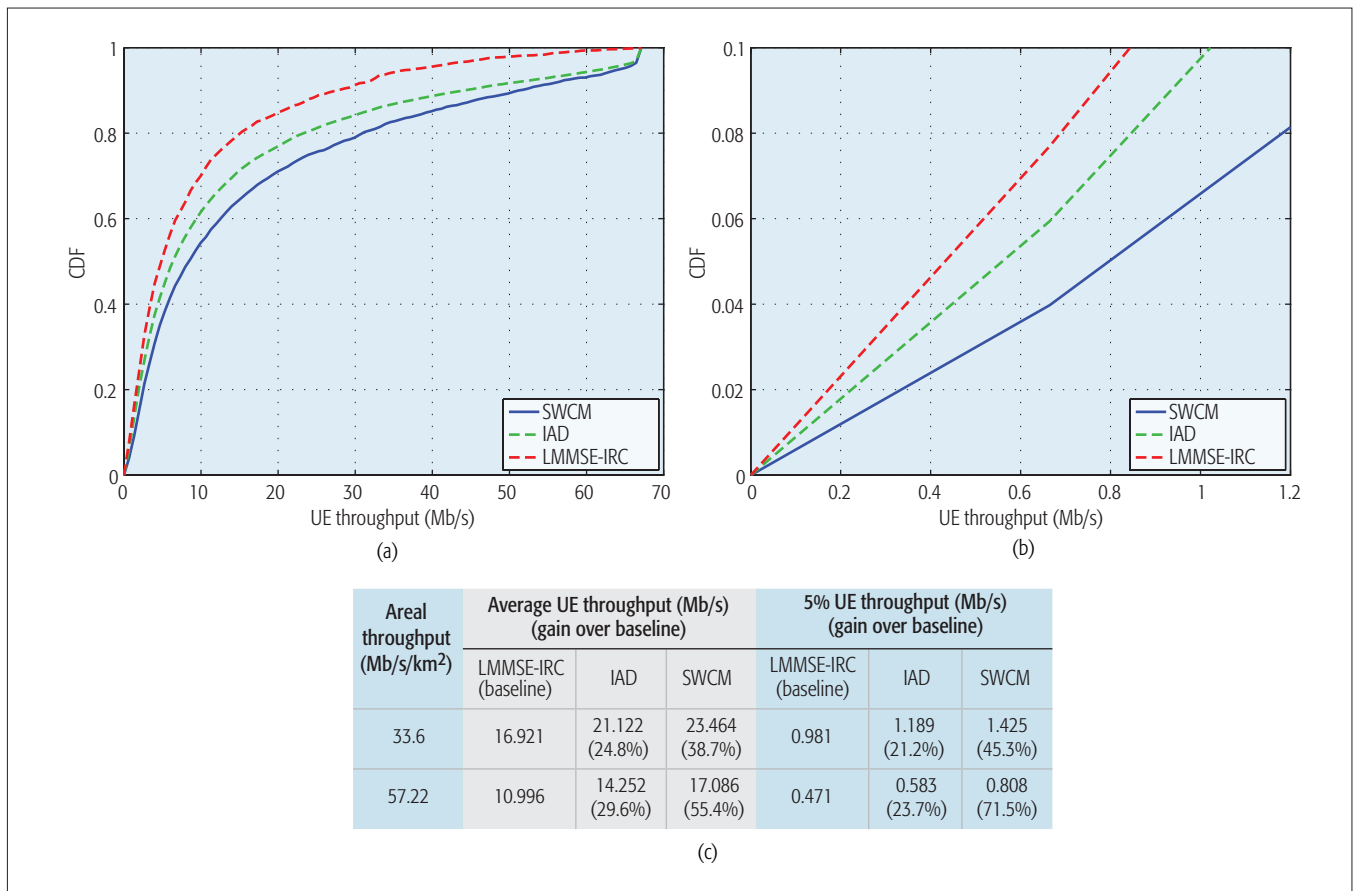


Figure 5. System-level performance in terms of the distribution of UE throughput for the 2/2-layer SWCM MIMO scheme, IAD, and LMMSE-IRC in the NAICS homogeneous scenario: a) UE throughput CDF; b) bottom 10 percent UE throughput CDF; c) summary.

(CQI), precoding matrix indicator (PMI), and rank indicator (RI) (with channel estimation errors reflected) to the TP at every predefined 5 ms interval, and feedback delay is also assumed to be 5 ms. Two LTE schemes (LMMSE-IRC and IAD) and SWCM are compared. UEs with LMMSE-IRC, IAD, or SWCM are configured to adapt PMIs and RIs according to the channel status. Two UEs in two different serving cells are paired for SWCM transmission based on PF scheduling metrics.

Figure 5 shows the cumulative distribution functions (CDFs) of cell-wide and cell-edge throughputs of the three schemes. SWCM achieves significant gains in both average UE throughput (the area above CDF) and cell-edge throughput (5th percentile CDF). SWCM outperforms LMMSE-IRC by 71.5 percent and IAD by 38.6 percent at the cell edge under areal throughput of 57.22 Mb/s/km<sup>2</sup> (or resource utilization of 54.44–63.94 percent). Note that user perceived throughput (during active time) is defined as the size of a burst divided by the time between its first packet arrival and its last packet reception. As for the average UE throughput, SWCM achieves gains of 55.4 percent and 19.9 percent over LMMSE-IRC and IAD, respectively, under the same areal throughput. As shown in Fig. 5c, the gain is more significant for the higher areal throughput environment, since UEs suffer from more severe co-channel interference.

## NETWORK OPERATING PREREQUISITES FOR SWCM

As a sequence-level interference-aware scheme, network-side supports are crucial for SWCM, since it requires information about interfering cells as well as the serving cell. Specifically, the SWCM scheme needs CSI feedback from a UE to a serving TP for multiple cooperating cells, joint scheduling over cooperating TPs for the SWCM transmission, a reference signal design for interfering channel estimation, and downlink control signaling for the SWCM decoding operation at UEs. Table 1 compares the requirements of different interference-aware transceiver techniques and the corresponding 3GPP standardization states.

### CHANNEL STATE INFORMATION FEEDBACK FOR MULTIPLE COOPERATING CELLS

For joint scheduling of multiple cells, it is important to infer the SWCM achievable rate region associated with each dominant interfering cell from CSI feedback. For this purpose, the UE reports to its serving TP the required CSI including RIs and PMIs associated with the combination of a serving cell and a particular interfering cell, and CQIs corresponding to corner points of the SWCM achievable rate region in Fig. 2a. There is an obvious trade-off between the amount of CSI reported (uplink control overhead) and the accuracy of the inferred achievable rate regions.

Changes from conventional networks	Required by				Standardized as
	LMMSE-IRC	IAD	IASD	SWCM	
CRS-associated information sharing for interference channel estimation	No	Yes	Yes	Yes	Release 12
PMI, RI, MCS, UE-specific RNTI sharing for interference decoding	No	No	Yes	Yes	N/A
Joint scheduling among TPs	No	No	Yes	Yes	Operator specific issue
A new Tx mode	No	No	No	Yes	N/A

**Table 1.** Prerequisites for interference-aware transceivers and standardization states.

### JOINT SCHEDULING OVER COOPERATING TPs

Joint scheduling is performed over the cooperating TPs based on the CSI feedback by comparing the inferred SWCM achievable rate regions of different pair combinations under fairness criteria. Since data sharing is not required to allocate resources jointly, to determine data rates and transmission schemes, or to perform link adaptation for the SWCM transmission, only CSI reports are shared over the X2 interface among cooperating TPs, requiring very small backhaul bandwidth compared to the conventional backhaul bandwidth necessary for data traffic.

Efficient joint scheduling typically relies on low-latency backhaul and CSI feedback. Thus, in order to maintain the full gain of the SWCM scheme, the network is responsible for meeting the latency requirement, in most cases one to three transmission time intervals (TTIs) due to hybrid automatic repeat request (HARQ) processing for 4G or 5G networks. Note that even under some loss due to feedback and backhaul latencies, the SWCM gain can be maintained to some extent since joint scheduling is performed based on the latest CSI reports from serving UEs, and each TP adjusts scheduling accordingly on the TTI basis. Long-term outer-loop rate control (OLRC) and UE-side techniques such as adaptive decoding in the earlier subsection can also alleviate the performance loss.

### DOWNLINK CONTROL AND REFERENCE SIGNALING

The SWCM reception procedure requires additional dynamic signaling besides higher-layer signaling supported in the 3GPP Release 12 NAICS for symbol-level interference management. This signaling requirement includes semistatic parameters (information that does not change often, once they are allocated) such as cell-specific reference signal antenna port (CRS AP), cell ID, data to RS energy per resource element (EPRE)  $P_A$  (UE-specific) and  $P_B$  (serving and interfering cell-specific) for channel estimation, system bandwidth, multicast-broadcast single-frequency network (MBSFN) configuration, resource allocation, precoding granularity information (1RB–4RB pairs), and transmission mode (TM1–TM9) associated with physical cell ID. Additional dynamic signaling may be carried by the downlink control information (DCI) message and consists of dynamic parameters (information

that may vary per subframe depending on the UE channel status) such as scheduling information jointly configured among the involved cells; MCS, PMI, RI, and radio network temporary identifier (RNTI) of the paired UE belonging to the interfering cell; and an indication of the use of SWCM transmissions. It is also crucial for a UE to estimate channels from interfering TPs as well as a serving TP in order to perform the SWCM reception and report CSI feedback to the serving TP for joint scheduling.

## CONCLUDING REMARKS

As one of the most advanced interference-aware communication techniques, the sliding-window coded modulation scheme closely tracks the performance of maximum likelihood sequence decoding at low complexity, effectively mitigating adverse effects of co-channel interference. Confirming previously reported theoretical gains, link-level and system-level performance simulations of our representative implementation under the current LTE OFDM MIMO system architecture demonstrate that SWCM offers significant gains in both cell average and cell edge throughput over conventional schemes at comparable decoding complexity, with a few feasible modifications of the conventional network operations. These results indicate that the SWCM scheme has promising potential to become a basic building block for interference management in 5G and subsequent generation cellular systems.

## ACKNOWLEDGMENTS

The authors would like to thank Lele Wang and Hosung Park for their earlier contributions and helpful discussions that led to the current work.

## REFERENCES

- [1] 3GPP TR 38.913, "Scenarios and Requirements for Next-Generation Access Technologies," v. 0.3.0, 2016.
- [2] 3GPP TR 25.963, "Feasibility Study on Interference Cancellation for UTRA FDD UE," v. 11.0.0, 2012.
- [3] Y. Ohwatori *et al.*, "Performance of Advanced Receiver Employing Interference Rejection Combining to Suppress Inter-Cell Interference in LTE-Advanced Downlink," *Proc. IEEE VTC-Fall*, San Francisco, CA, Sept. 2011, pp. 1–7.
- [4] 3GPP TSG-RAN WG1 Meeting #78, "R1-143535: LS for Rel-12 NAICS," Rel. 12, 2014.
- [5] J. Lee, D. Toumpakaris, and W. Yu, "Interference Mitigation via Joint Detection," *IEEE JSAC*, vol. 29, no. 6, June 2011, pp. 1172–84.
- [6] B. Bandemer, A. El Gamal, and Y.-H. Kim, "Optimal Achievable Rates for Interference Networks with Random Codes," *IEEE Trans. Info. Theory*, vol. 61, no. 12, Dec. 2015, pp. 6536–49.
- [7] A. Yedla *et al.*, "Universal Codes for the Gaussian MAC via Spatial Coupling," *Proc. 49th Annual Allerton Conf. Commun. Control Comp.*, Monticello, IL, Sept. 2011, pp. 1801–08.
- [8] L. Wang, and E. Sasoglu, "Polar Coding for Interference Networks," 2014, <http://arxiv.org/abs/1401.7293>.
- [9] J. Lee, H. Kwon, and I. Kang, "Interference Mitigation in MIMO Interference Channel via Successive Single-User Soft Decoding," *Proc. UCSD Info. Theory Appl. Workshop*, La Jolla, CA, Feb. 2012, pp. 180–85.
- [10] L. Wang, E. Sasoglu, and Y.-H. Kim, "Sliding-Window Superposition Coding for Interference Networks," *Proc. IEEE Int. Symp. Info. Theory*, Honolulu, HI, July 2014, pp. 2749–53.
- [11] L. Wang, *Channel Coding Techniques for Network Communication*, Ph.D. thesis, UCSD, 2015.
- [12] H. Park, Y.-H. Kim, and L. Wang, "Interference Management via Sliding-Window Superposition Coding," *Proc. Int'l. Wksp. Emerging Technologies for 5G Wireless Cellular Networks, IEEE GLOBECOM*, Austin, TX, Dec. 2014, pp. 1057–61.
- [13] K. T. Kim *et al.*, "Adaptive Sliding-Window Coded Modulation in Cellular Networks," *Proc. IEEE GLOBECOM*, San Diego, CA, Dec. 2015, 7 pp.
- [14] ITU-R Rec. M.1225, "Guidelines for Evaluation of Radio Transmission Technologies for IMT-2000," 1997.
- [15] 3GPP TS 36.211, "Physical Channels and Modulation," Release 12, 2013.

---

## BIOGRAPHIES

KWANG TAIK KIM [M] (kwangtaik.kim@samsung.com) received his B.S. degree in electrical engineering from Korea Advanced Institute of Science and Technology in 2001, and his M.S. and Ph.D. degrees in electrical and computer engineering from Cornell University in 2006 and 2008, respectively. He is currently a principal engineer in the Next Generation Communications Business Team at Samsung Electronics, where he does research on fifth generation cellular systems. He is a recipient of the 2014 Samsung CEO Award of Honor in the Technical Division. His research interests lie in information theory, and the fundamental and theoretical aspects of wireless and wireline communications.

SEOK-KI AHN (seokki.ahn@samsung.com) received his B.S., M.S., and Ph.D. degrees in electronics and electrical engineering from Pohang University of Science and Technology in 2006, 2008, and 2013, respectively. From 2010 to 2013, he was a student on scholarship at the Digital Media and Communications R&D Center of Samsung Electronics. Since 2013, he has been with Samsung Electronics as a senior engineer. His current research interests include channel coding, MIMO transceiver design, and broadband communications.

YONG-SEOK KIM (yongseok45.kim@samsung.com) received his M.S. degree in electrical engineering from Seoul National University, Korea, in 2004. In 2004, he joined Samsung Electronics, where he is currently a senior engineer in the Next Generation Communications Team. He worked on system designs and analysis for pre-4G trial (4x4 MIMO) systems, IEEE 16e/16m, and LTE systems. His current research interests include system designs and analysis for mmWave communications and new radio access technology in 5G.

JEONGHO PARK (jeongho.jh.park@samsung.com) received his B.S., M.S., and Ph.D. degrees in electronic engineering from Yonsei University in 1997, 2000, and 2005, respectively. Since he joined Samsung Electronics in 2005, he has mainly been engaged in research and development of wireless communications. Standardization is also his interest including IEEE 802, 3GPP RAN,

and ITU-R IMT-Systems. Currently, he is a director of the Next Generation Communications Business Team at Samsung Electronics and takes the lead in research and development of breakthrough technologies in 5G area.

CHIAO-YI CHEN (chc111@ucsd.edu) received his B.S. degrees in electrical engineering, and computer science and information engineering from National Taiwan University, Taipei, in 2006. During his undergraduate studies, he spent one year analyzing the impact of synchronization errors in CDMA systems with frequency domain equalization at Tohoku University, Japan. He received his M.S. degree in electrical and computer engineering from the University of California, San Diego (UCSD), and is pursuing his Ph.D. degree at the same university. He worked as an intern at Broadcom Corporation, Qualcomm Inc., and Blue Danube Systems. His research interests include information theory, communication theory, and universal processing. He received the 2002 National Taiwan University Presidential Award, the 2005 Japan Student Service Organization Scholarship, and the 2008 UCSD Electrical and Computer Engineering Departmental Fellowship.

YOUNG-HAN KIM [F] (yhk@ucsd.edu) received his B.S. degree with honors in electrical engineering from Seoul National University, Korea, in 1996, and his M.S. degrees in electrical engineering and statistics, and his Ph.D. degree in electrical engineering from Stanford University in 2001, 2006, and 2006, respectively. In 2006, he joined UCSD, where he is currently an associate professor of electrical and computer engineering. His research interests are in information theory, communication engineering, and data science. He coauthored the book *Network Information Theory* (Cambridge University Press, 2011). He is a recipient of the 2008 NSF Faculty Early Career Development (CAREER) Award, the 2009 U.S.-Israel Binational Science Foundation Bergmann Memorial Award, the 2012 IEEE Information Theory Paper Award, and the 2015 IEEE Information Theory Society James L. Massey Research and Teaching Award for Young Scholars. He served as an Associate Editor of *IEEE Transactions on Information Theory* and a Distinguished Lecturer for the IEEE Information Theory Society.